Hot electron energy relaxation via acoustic phonon emission in modulation-doped $In_{0.53}Ga_{0.47}As/In_{0.52}Al_{0.48}As$ heterojunctions with double-subband occupancy

E. Tiras, M. Cankurtaran, and H. Çelik
Hacettepe University, Faculty of Engineering, Department of Physics, Beytepe, 06532 Ankara, Turkey

N. Balkan
Semiconductor Optoelectronics Group, Department of Electronic Systems Engineering, University of Essex, Colchester, United Kingdom
(Received 8 February 2001; published 10 July 2001)

The energy relaxation associated with acoustic phonon emission in lattice-matched $In_{0.53}Ga_{0.47}As/In_{0.52}Al_{0.48}As$ heterojunctions, has been investigated using Shubnikov-de Hass (SdH) effect measurements performed in the temperature range from 3.3 to 25 K, and at electric fields up to 200 Vm^{-1}. The thickness (t_S) of the undoped spacer layer in modulation-doped samples was in the range between 0 and 400 Å . The SdH oscillations show that two subbands are populated for all samples except those with $t_S=400$ Å . The electron temperature (T_e) of hot electrons in each subband has been obtained from the lattice temperature (T_L) and applied electric field dependencies of the amplitude of SdH oscillations. For the samples with $t_S=0$, 100, and 200 Å , the power loss from the electrons in the first and second subbands is found to be proportional to (T_e^3-T_L^3) for electron temperatures in the range $3.3<T_e<12$ K, indicating that piezoelectric scattering is the dominant scattering mechanism. For the samples with $t_S=400$ Å , however, in which only the first subband is populated, the power loss is approximately proportional to (T_e-T_L) in the same range of electron temperatures. The experimental results are also compared with a three-dimensional model for electron energy loss by piezoelectric and deformation-potential scattering.

DOI: 10.1103/PhysRevB.64.085301 PACS number(s): 73.40.Kp, 73.50.Jt, 73.43.Qt

I. INTRODUCTION

The energy relaxation of hot carriers in semiconductors has been investigated extensively, both experimentally and theoretically in bulk and two-dimensional (2D) structures (for review see[1–3]). The determination of the temperature of electrons, under electric-field heating conditions in the steady state, provides useful information about the electron-phonon interactions involved in the energy relaxation process. Since at temperatures below about 30–40 K, the population of optical phonons is negligibly small, acoustic phonon scattering provides the only inelastic-scattering mechanism.[3–6]

Most of the previous experimental investigations of power loss in 2D electron-gas systems, in the acoustic phonon regime, were performed on modulation-doped $GaAs/Ga_{1-x}Al_xAs$ heterojunctions and quantum well structures, in which only the lowest subband was populated by electrons and hence all the scattering processes were of an intrasubband nature.[7–21] A substantial increase in the 2D carrier density, moving the Fermi level above the second subband, would give rise to inelastic intersubband scattering processes, which may affect the overall energy relaxation rates.[14,15] The first experiments devoted to study the acoustic phonon assisted power loss in a 2D electron gas with double-subband occupancy, were carried out for modulation-doped $GaAs/Ga_{1-x}Al_xAs$ heterostuctures, where the carrier density was varied by using the persistent photoconductivity effect.[14,15,18,22,23]

Comparatively little work have been published in the literature concerning measurements of the power loss of hot electrons in material systems, where the 2D electron gas is confined in the $In_{0.53}Ga_{0.47}As$ ternary alloy.[13,17,24–27] To our knowledge, there is no study to date concerning the acoustic phonon assisted energy relaxation of hot electrons in the $In_{0.53}Ga_{0.47}As/In_{0.52}Al_{0.48}As$ heterojunctions with double-subband occupancy. In the present work we have investigated energy relaxation in modulation-doped $In_{0.53}Ga_{0.47}As/In_{0.52}Al_{0.48}As$ heterojunctions, lattice-matched to InP substrates, in which one or two subbands are populated by electrons, depending on the thickness (t_S) of the undoped spacer layer. We present the results of Shubnikov–de Haas (SdH) effect measurements in samples with spacer layer thickness in the range between $t_S=0$ and 400 Å. In all but in the samples with $t_S=400$ Å, the first two subbands are already occupied at liquid-He temperatures. The temperature of hot electrons (T_e) in each subband of the samples and the corresponding power loss (P), have been determined as a function of the applied electric field. The results are discussed in the framework of the current theoretical models concerning carrier energy-loss rates in semiconductors.

The SdH oscillations in magnetoresistance, provide an accurate and sensitive technique that has been employed successfully in the investigations of electron energy relaxation in the acoustic phonon regime.[19,21,28–31] In heavily modulation-doped structures, where a highly-degenerate electron gas exists, the variations of the amplitude of the SdH oscillations with applied electric field and lattice temperature, can be used in the determination of the power loss, electron temperature characteristics. All the samples used in the present paper are highly degenerate, so that the reduced Fermi energy $\eta=(E_F-E_i)/k_BT\gg 1$ (Table I), even at electron temperatures of about 30 K, which is well above the range of temperatures considered here. Therefore, we employed the

TABLE I. Sample parameters, electronic and transport properties of the modulation-doped $In_{0.53}Ga_{0.47}As/In_{0.52}Al_{0.48}As$ heterojunctions determined at 3.3 K.

Sample	MV572A		MV576A		MV577		MV578A
Spacer thickness, t_S(Å)	0		100		200		400
Subband Index	First	Second	First	Second	First	Second	First
2D carrier density, N_i (10^{16} m^{-2})	1.67 ± 0.05	0.33 ± 0.01	1.09 ± 0.005	0.21 ± 0.005	0.86 ± 0.01	0.12 ± 0.01	0.51 ± 0.001
Total 2D carrier density, N_1+N_2 (10^{16} m^{-2})	2.00 ± 0.05		1.30 ± 0.007		0.98 ± 0.01		0.51 ± 0.001
Hall carrier density, N_H (10^{16} m^{-2})	1.95 ± 0.05		1.10 ± 0.04		0.91 ± 0.02		1.13 ± 0.03
Effective mass, m^* (m_0)	0.039 ± 0.001		0.041 ± 0.001	0.037 ± 0.002	0.039 ± 0.001		0.042 ± 0.001
Fermi Energy, E_F-E_i (meV)	102 ± 4	20.5 ± 0.5	64 ± 2	13.5 ± 0.4	53 ± 2	7.6 ± 0.2	29.1 ± 0.8
E_2-E_1 (meV)	82 ± 4		51 ± 2		45 ± 2		
Hall mobility, μ_H (m^2 V^{-1} s^{-1})	4.8 ± 0.1		8.1 ± 0.2		6.7 ± 0.2		4.1 ± 0.1
Transport mobility, μ_{ti} (m^2 V^{-1} s^{-1})	4.91	3.75	7.54	3.30	6.92	1.08	9.16
Quantum lifetime, τ_{qi} (10^{-12} s)	0.20 ± 0.007		0.15 ± 0.01	0.25 ± 0.01	0.17 ± 0.01		0.42 ± 0.03
γ	3.2		3.1	3.4	3.1		≈1
A (eV s^{-1} $K^{-\gamma}$)	9		25	6	28		

SdH oscillations technique in our investigations. The method is based on the assumption that ionized-impurity scattering, alloy scattering, and interface roughness scattering, which determine the low-temperature transport mobility of electrons, are elastic in nature. Consequently, the energy that is gained by electrons in an applied electric field, is dissipated via the emission of acoustic phonons.

The SdH oscillations in magnetoresistance of a 2D electron gas of single-subband occupancy, are well described by the analytic function[32–35]

$$\frac{\Delta\rho_{xx}}{\rho_0}\propto D(\chi)\exp\left(\frac{-\pi}{\omega_c\tau_q}\right)\cos\left[\frac{2\pi(E_F-E_1)}{\hbar\omega_c}-\pi\right], \quad (1)$$

where $\Delta\rho_{xx}$, ρ_0, E_F, E_1, $\omega_c(=eB/m^*)$, m^*, and τ_q are the oscillatory magnetoresistivity, zero magnetic-field resistivity, Fermi energy, first-subband energy, cyclotron frequency, effective mass, and quantum lifetime of 2D electrons in the first subband, respectively. The effects of higher harmonics are neglected in Eq. (1).[28,36] The formula in Eq. (1) was originally derived[32–34] for carrier transport in a 2D electron gas of single-subband occupancy under the condition $\omega_c\tau_q\leqslant1$. However, this condition is not stringent and Eq. (1) describes well the experimental SdH oscillations data for all $\omega_c\tau_q$ values as long as $\Delta\rho_{xx}<\rho_0$ (see Refs. 19,35,37–39). The exponential term, $\exp(-\pi/\omega_c\tau_q)$, describes the damping due to the collision broadening of the Landau levels. The temperature dependence of the envelope function of the SdH oscillations is totally contained in the term

$$D(\chi)=\frac{\chi}{\sinh\chi} \quad (2)$$

with

$$\chi=\frac{2\pi^2k_BT}{\hbar\omega_c},$$

where $\hbar$ is the Planck's constant and k_B is the Boltzmann constant. The thermal damping of the amplitude of the SdH oscillations is, therefore, determined by the temperature, magnetic field, and effective mass via

$$\frac{A(T,B_n)}{A(T_0,B_n)}=\frac{T\sinh(2\pi^2k_BT_0m^*/\hbar eB_n)}{T_0\sinh(2\pi^2k_BTm^*/\hbar eB_n)}, \quad (3)$$

where $A(T,B_n)$ and $A(T_0,B_n)$ are the amplitudes of the oscillation peaks observed at a magnetic field B_n and at temperatures T and T_0. In the derivation of Eq. (3) from Eq. (1), it has been assumed that the quantum lifetime (τ_q) is independent of both temperature and magnetic field. The quantum lifetime can be determined from the magnetic-field dependence of the amplitude of the SdH oscillations (i.e., Dingle plots) at a constant temperature provided that the electron effective mass is known[28,29,36]

$$\ln\left[\frac{A(T,B_n)B_n^{-1/2}\sinh(\chi)}{\chi}\right]=C-\frac{\pi m^*}{e\tau_q}\frac{1}{B_n}, \quad (4)$$

where C is a constant.

GaAs	undoped	50 Å
$In_{0.52}Al_{0.48}As$	$n^+ \sim 10^{24}$ m^{-3} (Si)	250 Å
$In_{0.52}Al_{0.48}As$	undoped	(t_S=0, 100, 200, and 400 Å)
$In_{0.53}Ga_{0.47}As$	undoped	6000 Å
$In_{0.53}Ga_{0.47}As$ InP (Fe) substrate	$p \sim 10^{23}$ m^{-3} (Be) Semi-insulating	2000 Å

FIG. 1. The structure of the modulation-doped $In_{0.53}Ga_{0.47}As/In_{0.52}Al_{0.48}As$ heterojunctions samples used in the paper.

In the case of a 2D electron gas of double-subband occupancy, the quantum oscillations in magnetoresistance can be represented by a weighted sum of contributions from all the populated subbands:[21,40–42]

$$\frac{\Delta\rho_{xx}}{\rho_0} \propto \sum_{i=1}^{n} D(i,\chi)\exp\left(\frac{-i\pi}{\omega_c\tau_q}\right)\cos\left[\frac{2i\pi(E_F-E_i)}{\hbar\omega_c}-i\pi\right], \tag{5}$$

where the subscript i labels the populated subbands.

Assuming that the change in the SdH amplitude with applied electric field can be described in terms of electric-field induced electron heating, the temperature T in Eqs. (1) to Eq. (5) can be replaced by the electron temperature T_e. Therefore, T_e can be determined by comparing the relative amplitudes of the SdH oscillations measured as functions of the lattice temperature ($T=T_L$) and the applied electric field (F) using[21,28,29]

$$\left[\frac{A(T_L,B_n)}{A(T_{L0},B_n)}\right]_{F=F_0} = \left[\frac{A(F,B_n)}{A(F_0,B_n)}\right]_{T_L=T_{L0}}. \tag{6}$$

Here $A(F,B_n)$ and $A(F_0,B_n)$ are the amplitudes of the oscillation peaks observed at a magnetic field B_n and at electric fields F and F_0, respectively. In order to obtain the electron temperature from the lattice temperature and electric-field dependencies of the amplitude of the SdH oscillations, the quantum lifetime has to be independent of both the lattice temperature and the applied electric field.

II. EXPERIMENTAL PROCEDURES

The modulation-doped $In_{0.53}Ga_{0.47}As/In_{0.52}Al_{0.48}As$ heterojunctions were grown by the molecular beam epitaxy technique. During the growth, sample parameters including doping density, alloy fractions, and layer thicknesses are estimated from the calibrated charts for the specific growth conditions and materials. After the growth, these parameters were measured for each wafer, using standard characterization techniques such as photoluminescence, scanning transmission electron spectroscopy, and capacitance-voltage profiling, and energy dispersive x-ray analysis. The samples were fabricated in Hall-bar geometry and Ohmic contacts were formed by diffusing the Au/Ge/In alloy. The layer structure and doping parameters of all the samples (Fig. 1) were nominally identical with the exception of the thickness (t_S) of the undoped $In_{0.52}Al_{0.48}As$ spacer layer, which was varied from 0 (no spacer layer) to 400 Å. Table I lists the growth characteristics and the electronic and transport parameters of all the samples studied, which include structures with both single- and double-subband occupancy.

The magnetoresistance measurements were carried out as functions of (i) the applied electric field at a fixed lattice temperature T_{L0} (the lowest of the lattice temperature range) and (ii) the lattice temperature ($T_{L0}<T_L<25$ K) at a fixed electric field F_0, which was low enough to ensure Ohmic conditions and hence to avoid carrier heating. The magnetoresistance measurements were performed in a three-stage closed-cycle refrigeration system (HS-4 Heliplex, APD Cryogenics) using a conventional dc technique in combination with a constant current source (Keithley 220) and a nanovoltmeter (Keithley 182). The current flow was in the plane of the 2D electron gas. Steady magnetic fields (B) up to 2.3 T were applied perpendicular to the plane of the samples and hence to the plane of the 2D electron gas. The data were taken at equal intervals of $1/B$. All the measurements were performed in the dark.

III. RESULTS AND DISCUSSION

Figures 2(a) and 2(b) show typical examples for the magnetoresistance (R_{xx}) measurements in the modulation-doped $In_{0.53}Ga_{0.47}As/In_{0.52}Al_{0.48}As$ heterojunctions sample with $t_S=100$ Å for different lattice temperatures at a fixed electric field $F_0=3.84$ Vm^{-1}, and for different electric fields at a fixed lattice temperature $T_{L0}=3.28$ K, respectively. The data clearly show the decrease in the amplitude of the SdH oscillations with increasing lattice temperature or electric field. It is evident from Figs. 2(a) and 2(b) that the oscillatory component of the magnetoresistance consists of two superimposed sets of oscillations with different periods indicating the occupation of two subbands.[23,42,43] This is also true for the samples with $t_S=0$ and 200 Å (see Ref. 44). Fourier transform of the raw $R_{xx}(B)$ data for the samples with $t_S=0$, 100, and 200 Å yields two peaks confirming that two subbands are populated in these samples. For the sample with $t_S=400$ Å, however, the SdH oscillations contain only one period (i.e., only the lowest subband is populated) and are superimposed on a positive background magnetoresistance [Figs. 3(a) and 3(b)]. It has been shown in Ref. 44 that the strong positive magnetoresistance measured for this sample is due to the parallel conduction in the Si-doped $In_{0.52}Al_{0.48}As$ barrier.

In order to separate the oscillatory components with different periods, the second-derivative technique and digital filtering have been employed. The second-derivative technique removes the effects of the background magnetoresistance, which varies slowly with magnetic field, suppresses the amplitude of the long-period oscillations, and amplifies that of the short-period oscillations.[37,44,45] The SdH oscillations associated with the first subband are extracted by directly calculating the negative second derivative ($-\partial^2 R_{xx}/\partial B^2$) of the raw experimental data with respect to the magnetic field. To separate the SdH oscillations associated with the second subband, suitable low-pass digital fil-

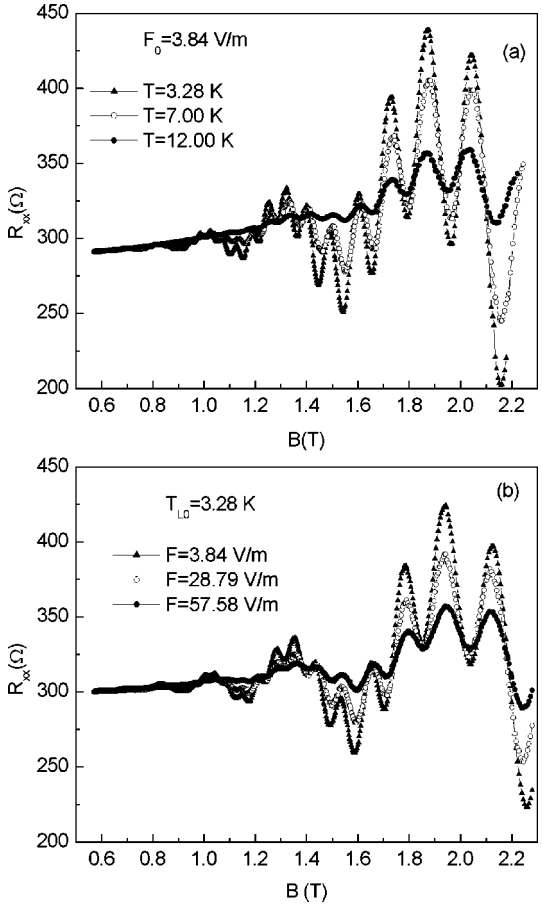

FIG. 2. Experimental results showing the effects of (a) temperature and (b) applied electric field on the magnetoresistance $R_{xx}(B)$ measured for sample MV576A ($t_S = 100$ Å) in which two subbands are populated by electrons.

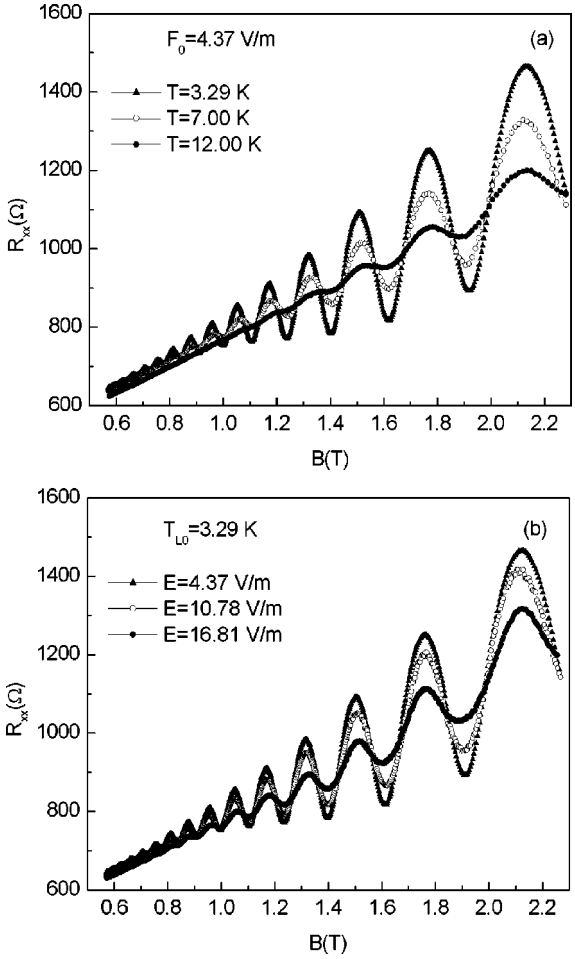

FIG. 3. Experimental results showing the effects of (a) temperature and (b) applied electric field on the magnetoresistance $R_{xx}(B)$ measured for sample MV578A ($t_S = 400$ Å) in which only the lowest subband is populated by electrons.

tering has been first applied to the raw $R_{xx}(B)$ data and then $-\partial^2 R_{xx}/\partial B^2$ has been calculated. For further details of data analysis, refer to Ref. 44. Typical plots of the two oscillatory components, as extracted from the $R_{xx}(B)$ data for the sample with $t_S = 100$ Å , are shown in Figs. 4(a)–4(d). Both series of SdH oscillations could be isolated completely. The SdH oscillations associated with each subband have well-defined envelopes and can be represented by Eq. (1). The SdH oscillations similar to those given in Figs. 4(a)–4(d), have been analyzed to yield the electronic transport properties and power loss electron temperature characteristics appropriate to the individual subbands in the samples with double-subband occupancy.

The carrier density (N_i) in each subband, the Fermi energy with respect to the subband energy (E_F-E_i), the energy separation of the two populated subbands (E_2-E_1), the in-plane effective mass (m^*) and the quantum lifetime (τ_q) of 2D electrons, as determined[44] from the analysis of the SdH oscillations measured under cold electron conditions, are summarized in Table I. The transport mobility (μ_t) of 2D electrons in each subband of the samples (Table I) has been determined from magnetoresistance measurements in the classical regime.[44] For the samples with double-subband occupancy, the total carrier density of 2D electrons, determined independently from the SdH oscillations and Hall effect measurements, are in good agreement. This indicates that any parallel conduction due to carriers outside the 2D channel is negligible for these samples at low temperatures. The in-plane effective mass of 2D electrons in each subband of all the samples is practically independent of magnetic field in the range from 0.8 to 2.3 T. The carrier density, quantum lifetime, and transport mobility of 2D electrons in each subband are found to be essentially independent of both the lattice temperature in the range from 3.3 to 15 K and the applied electric field up to 120 Vm^{-1}.

It can be seen from Figs. 2–4 that increasing the lattice temperature (T_L) or the applied electric field (F) results in the damping of the amplitude of the SdH oscillations. Figures 5 and 6 show the amplitudes of the SdH oscillations, normalized, as described by Eq. (6), as functions of T_L and F for the samples with $t_S = 100$ and 400 Å , respectively. The relative amplitude of the SdH oscillations decreases with increasing T_L (or F) in accordance with the thermal damping factor given in Eq. (2). In the figures, only the relative amplitudes at a given magnetic field B_n are shown for clarity. A similar analysis made for all the SdH peaks observed in the

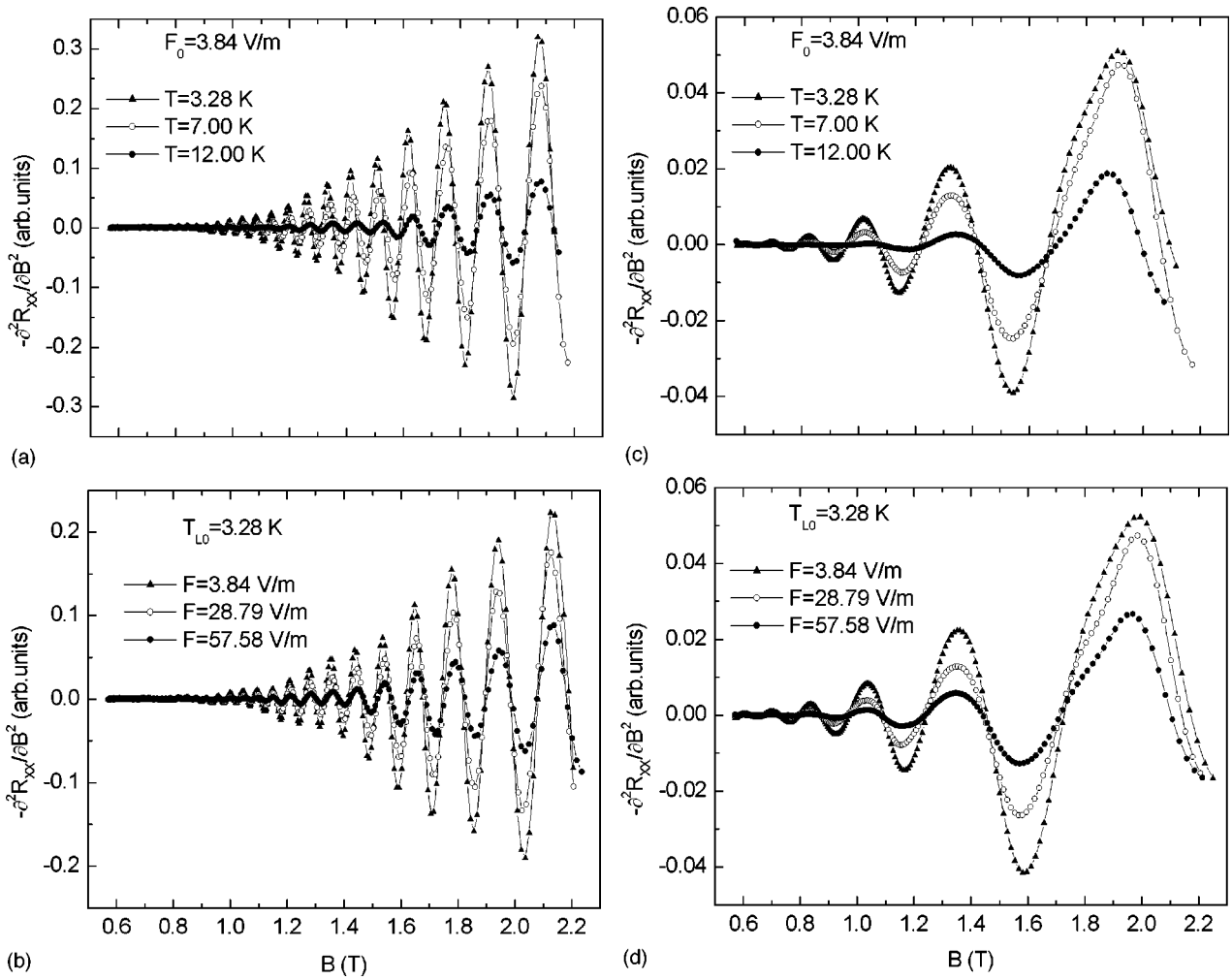

FIG. 4. The effects of temperature (upper panel) and applied electric field (lower panel) on the SdH oscillations arising from the electrons in the first [(a) and (b)] and second [(c) and (d)] subbands, as extracted from the $R_{xx}(B)$ data for sample MV576A ($t_S = 100$ Å) shown in Fig. 2. The full curves through the experimental data points are intended as a guide to the eye.

magnetic field range from 0.8 to 2.3 T has established that the relative amplitudes of SdH oscillations (and hence the electron temperatures) in our samples are essentially independent of magnetic field. This indicates that the magnetic field used in our experiments does not alter significantly the energy relaxation processes of hot electrons. Although we have observed well-resolved SdH oscillations in all the samples with double-subband occupancy at lattice temperatures up to about 25 K or applied electric fields up to about 200 Vm^{-1}, the data obtained in the ranges $T_L > 15$ K and $F > 120$ Vm^{-1} are not used in the determination of the electron temperature. This is because, at higher lattice temperatures or electric fields, the relative amplitude of the SdH oscillations decreases to less that 10% of the initial value and the rate of change in relative amplitude with T_L or F becomes very small (see Fig. 5), so that the experimental resolution reduces and hence the evaluation of T_e becomes gradually unreliable.

It should be noted that the determination of the electron temperature T_e from the lattice temperature and electric-field dependencies of the amplitude of SdH oscillations becomes complicated in the samples where two subbands are populated. It has been possible to extract quantitative information about the power loss characteristics of hot electrons in both the first and second subbands of the sample with $t_S = 100$ Å. However, the amplitude of the short-period component of the oscillations originating from the first subband of the sample with $t_S = 0$ Å, was much smaller compared to that of the long-period oscillations associated with the second subband and diminished with increasing lattice temperature or the applied electric field. We were, therefore, able to determine T_e of electrons only in the second subband of this sample. Because of the lack of prominent oscillation peaks from the second subband of the sample with $t_S = 200$ Å, the electron temperature can only be obtained for the first subband.

The electron temperature associated with each populated subband in the modulation-doped $In_{0.53}Ga_{0.47}As/In_{0.52}Al_{0.48}As$ heterojunctions, as obtained by comparing directly the curves similar to those in Figs. 5(a) and 5(b) [and Figs. 6(a) and 6(b)], is plotted as a function of the applied electric field in Fig. 7 for all the samples studied. It can be seen from the figure that, for the sample with $t_S = 100$ Å, the electron temperatures determined separately for the electrons

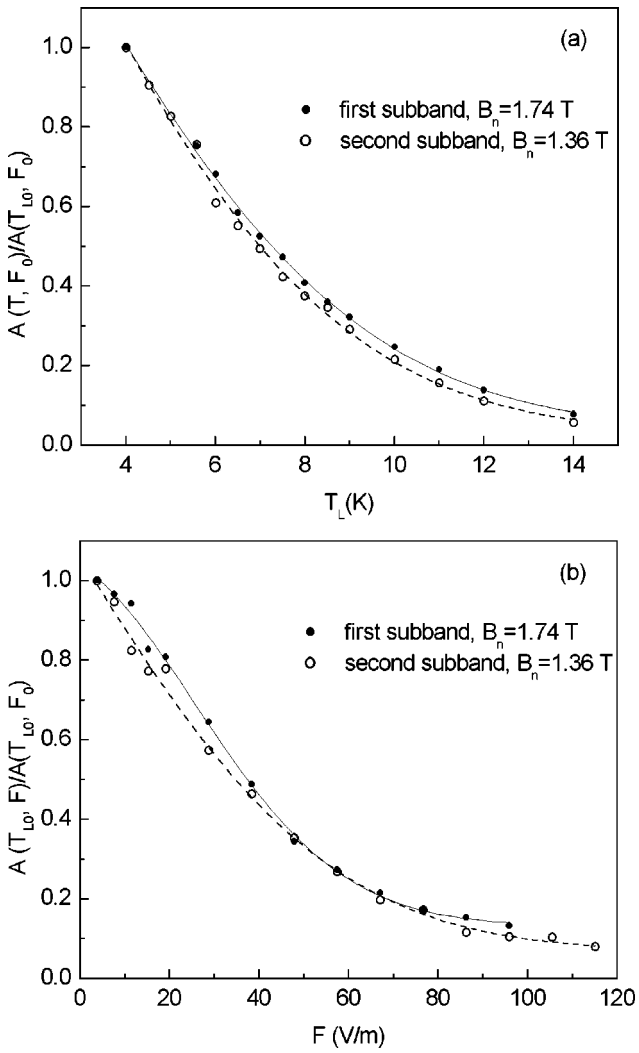

FIG. 5. (a) Temperature and (b) electric-field dependencies of the normalized amplitude of the oscillation peak at B_n measured for sample MV576A ($t_S = 100$ Å). The data points represented by the full circles and open circles correspond to the SdH oscillations arising from the electrons in the first and second subbands, respectively. The full and dashed curves are the best fits of Eq. (3) to the experimental data for the first and second subbands, respectively.

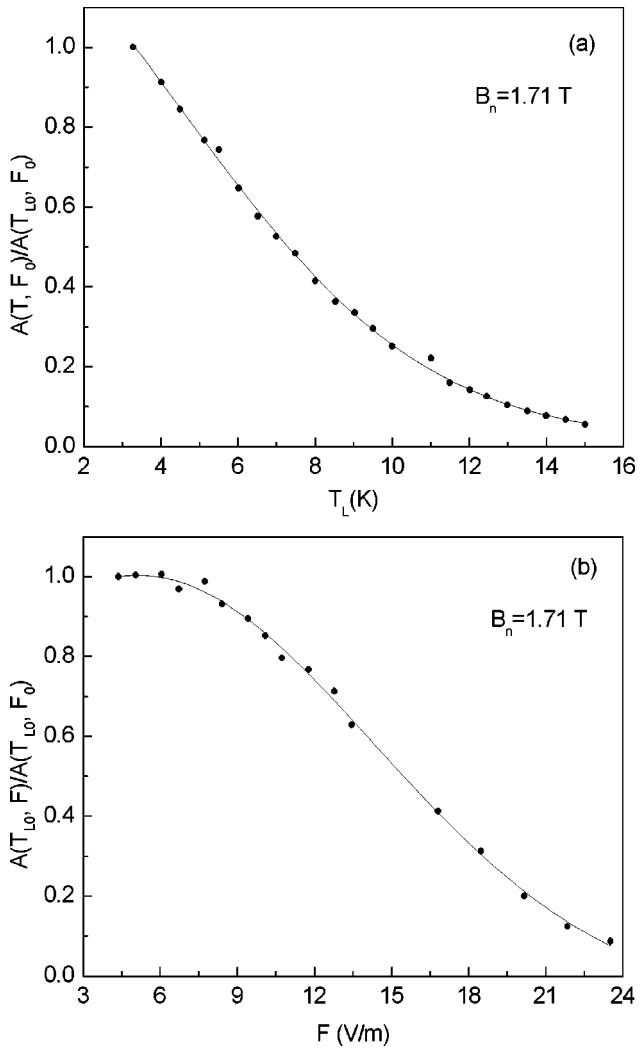

FIG. 6. (a) Temperature and (b) electric-field dependencies of the normalized amplitude of the oscillation peak at B_n measured for sample MV578A ($t_S = 400$ Å). The full circles correspond to the experimental data and the full curve is the best fit of Eq. (3) to the experimental data.

in the first and second subbands are identical within the experimental error due to the complex pattern of the SdH oscillations. This shows that the electrons in the two subbands are in thermal equilibrium with each other, as would be expected from electron-electron scattering on a time scale that is orders of magnitude less than the energy relaxation time,[2,3,18,23] so that the 2D electron gas itself represents a system in thermal equilibrium characterized by an electron temperature T_e greater that the lattice temperature T_L. The electron temperatures determined for all the samples are found to be practically independent of magnetic field in the range from 0.8 to 2.3 T. This result is in line with that found for modulation-doped GaAs/$Ga_{1-x}Al_xAs$ heterojunctions, where only the first subband was populated.[19,22,23] Recently, however, Leadley *et al.*[18] reported that, when the applied electric field was increased above about 5 Vm^{-1}, the electron temperature determined for high-mobility GaAs/$Ga_{1-x}Al_xAs$ heterojunctions, developed a strong dependence on magnetic field in the range below about 0.8 T, and suggested it to be due to cyclotron phonon emission (see also Ref. 19).

The SdH oscillations measured for the sample with $t_S = 400$ Å, decrease rapidly when increasing the applied electric field and become vanishingly small for $F > 30$ Vm^{-1} [see Figs. 3(b) and 6(b)]. The electron temperature determined for this sample, rises quickly with increasing F, reaching 15 K when $F \cong 25$ Vm^{-1} (Fig. 7). The 2D electrons in this sample are easily heated by a relatively small electric field, possibly due to their higher transport mobility when compared with the samples of double-subband occupancy (Table I).

In the steady state, the power loss from hot electrons by the emission of acoustic phonons is equal to the power supplied by the applied electric field, which can be calculated using the energy balance equation[1,28,46]

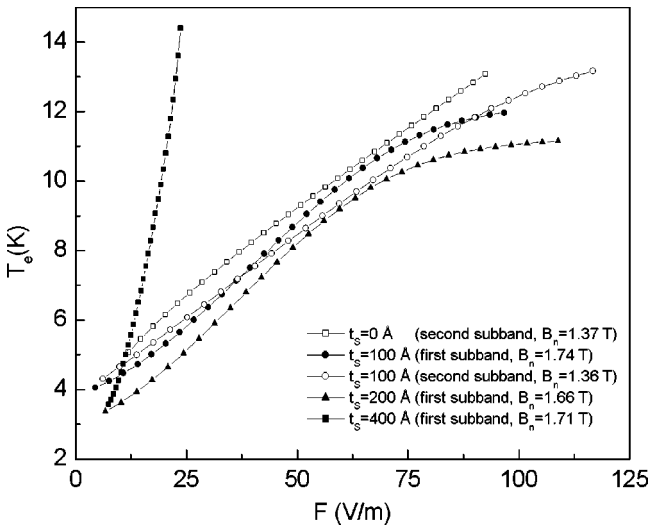

FIG. 7. Electron temperature (T_e) versus applied electric field (F) for all the samples studied. The full curves through the experimental data points are intended as a guide to the eye.

$$P = e\mu_t F^2, \tag{7}$$

where P, μ_t, and F are the energy loss (or energy supply) rate per electron, transport mobility, and applied electric field, respectively. The transport mobility of 2D electrons in modulation-doped $In_{0.53}Ga_{0.47}As/In_{0.52}Al_{0.48}As$ heterojunction samples has been found to be essentially independent of both the lattice temperature and applied electric field in the ranges of interest, since it is determined mainly by alloy-disorder scattering and ionized impurity scattering,[44,47] which lead to momentum relaxation of electrons but not energy relaxation to the lattice. In the calculations of power loss, therefore, we used the transport mobilities as given in Table I. The power loss versus electron temperature is plotted in Fig. 8 for all the samples studied. The magnitude of the power loss varies significantly from one sample to another. Since the layer structures and doping parameters of all the samples are identical (Fig. 1), the observed variations in power loss may be associated with the differences in spacer thickness (and hence 2D carrier density) of the samples.

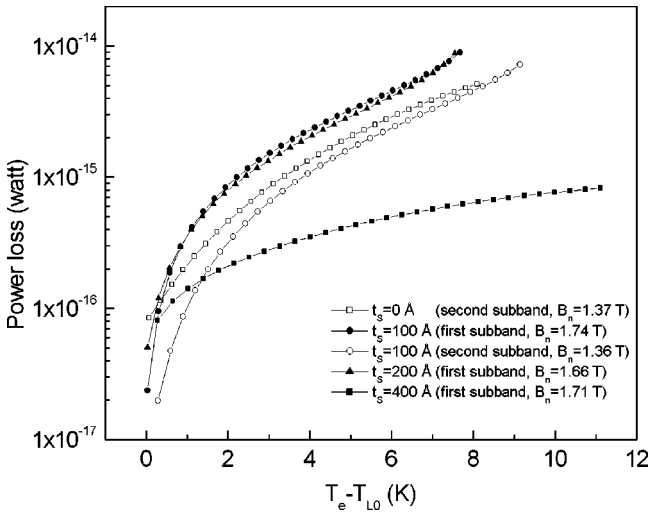

FIG. 8. Power loss per electron versus T_e-T_{L0} for all the samples studied. The full curves through the experimental data points are intended as a guide to the eye.

The variation of the power loss per electron with electron temperature has been often approximated by the relationship

$$P = A(T_e^{\gamma} - T_{L0}^{\gamma}), \tag{8}$$

where the proportionality constant A depends on the elastic moduli of the matrix, the coupling constants, and the 2D carrier density. Theoretical calculations of the acoustic phonon assisted energy loss rates of hot electrons in a 2D electron gas of single-subband occupancy, predict $\gamma=1$ at high temperatures (when Maxwell-Boltzmann statistics is applicable and equipartition is assumed) and $\gamma=3$ (unscreened piezoelectric scattering), $\gamma=5$ (unscreened deformation potential and heavily-screened piezoelectric scatterings), and $\gamma=7$ (heavily-screened deformation potential scattering) at low temperatures (see for instance Refs. 3,11,14,15,23,48, 49).

For the modulation-doped $In_{0.53}Ga_{0.47}As/In_{0.52}Al_{0.48}As$ heterojunction samples with spacer thickness $t_S=0$, 100, and 200 Å , we found that $\gamma\cong 3$ for each populated subband (see Table I) by fitting Eq. (8) to the experimental data (Fig. 9). In all cases a constant value for the exponent γ is obtained over the whole temperature range from 3.3 to 12 K. This result is consistent with the theoretical predictions that the main energy loss mechanism is the scattering of hot electrons by the piezoelectric potential of acoustic phonons. The effect of screening of the electron acoustic phonon interaction by 2D electrons, is expected to increase towards low temperatures for samples with high carrier density, as the scattering of acoustic modes involves smaller and smaller wave vectors.[4,6] Although the 2D carrier density in our samples is large enough so that the screening is anticipated to be effective, we found no evidence for a higher value of the exponent γ, as $(T_e\text{-}T_{L0})\rightarrow 0$. One could also consider that the temperature range of our experiments is intermediate between the low-temperature (Bloch-Grüneisen) and high-temperature (equipartition) limits.[18,19,23] For modulation-doped $In_{0.53}Ga_{0.47}As/InP$ heterojunctions and single quantum wells of single-subband occupancy, Barlow *et al.*[13] found an exponent between 3 and 5, for electron temperatures in the range from 2 to 20 K, which was explained by assuming that energy relaxation is due to acoustic phonon emission via mixed unscreened piezoelectric and deformation potential interactions (see also Ref. 27). However, for the modulation-doped $In_{0.53}Ga_{0.47}As/In_{0.52}Al_{0.48}As$ heterojunctions sample with $t_S=400$ Å , in which only the lowest subband is populated, we found that the power loss is approximately proportional to $(T_e\text{-}T_{L0})$. A linear dependence of power loss on electron temperature was reported previously for a weakly degenerate 2D electron gas in modulation-doped $In_{0.53}Ga_{0.47}As/In_{0.52}Al_{0.48}As$ heterojunctions in the lattice temperature range $3<T_L<20$ K,[17] and for $In_{0.53}Ga_{0.47}As/InP$ and $(InGa)_1(GaAs)_1/InP$ heterojunctions at electron temperatures below 10 K.[25] The linear behavior is in accord with the theoretical predictions for the variation of power loss with

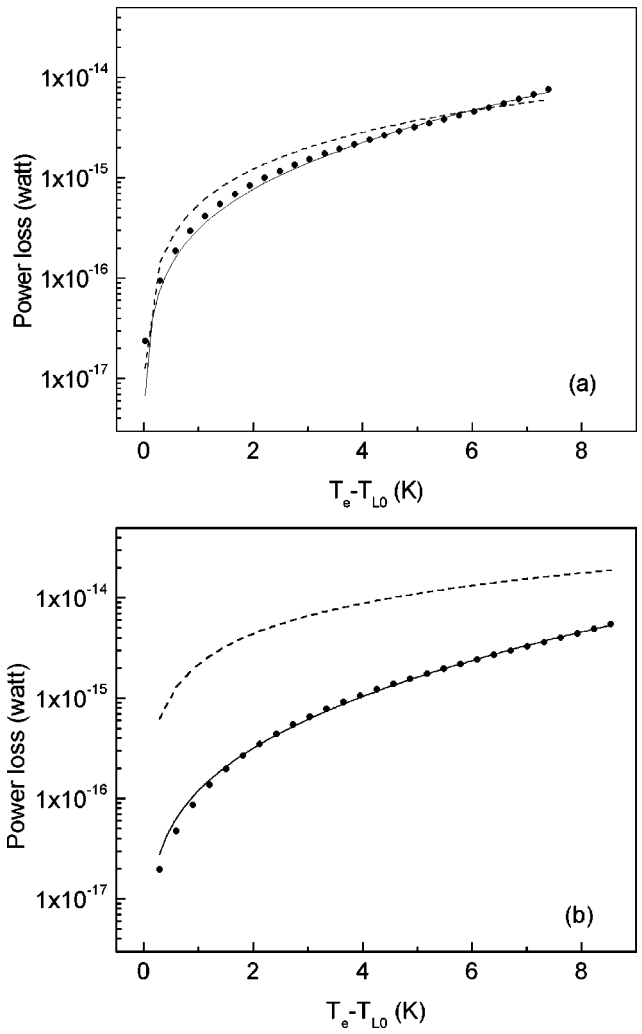

FIG. 9. Comparison of the experimental power loss determined for the (a) first and (b) second subbands in sample MV576A ($t_S = 100$ Å) with theory. The full circles represent the experimental data. The full curve corresponds to the best fit of Eq. (8) to the experimental data points and the dashed curve to the power loss calculated using Eq. (9) (see text).

electron temperature for a 2D electron gas in the equipartition regime. However, as pointed out by Ridley,[3] the experimental observation that $P \propto (T_e\text{-}T_{L0})$ may also be an indication of the influence of parallel conduction in the barrier, which is present in our sample with $t_S = 400$ Å (see Ref. 44). If the parallel conduction is significant, energy relaxation in the 2D channel may be affected by electron-electron interactions between the electrons in the 2D channel and those in the barrier.[16]

Theoretical calculations of the energy loss rate in the acoustic phonon regime were also made[14] for the case of a 2D electron gas with double-subband occupancy by assuming that the electrons in both subbands are described by a Fermi-Dirac distribution function with the same Fermi level E_F and with the same electron temperature T_e. In this case the total energy loss rate consists of four terms, $P = P_{11} + P_{12} + P_{21} + P_{22}$, where P_{ij} is the energy loss rate of hot electrons in the ith subband, which are transferred to the jth subband as a result of electron-phonon scattering.[14,15] As mentioned above, formulae for $P_{11}(T_e)$ were derived by many researchers (see, for instance,[4,6,10,23,48,49]) by considering the energy relaxation in the presence of one populated subband. The expressions derived[14] for the electron-temperature dependencies of the intersubband scattering processes P_{12} and P_{21}, are rather complex and differ from the simple power-law behavior of P_{11} with T_e.

In the case of low temperatures and weak heating such that $k_B T_e \ll [8m^* V_S^2 (E_2\text{-}E_1)]^{1/2}$, a condition that is satisfied to a large extent in our experiments, Kreshchuk *et al.*,[14] showed that $P_{12} \sim P_{21} \propto \exp(-[8m^* V_S^2 (E_2\text{-}E_1)]^{1/2}/k_B T_e)$, where V_S is the sound velocity. For 2D electron-gas structures with large subband separation, $(E_2\text{-}E_1) \gg k_B T_e$, which is the case for all our samples with double-subband occupancy (see Table I), the inelastic intersubband scattering is expected to be greatly suppressed when compared with the intrasubband scattering. It is well known that a minimum phonon wave vector and a corresponding minimum phonon energy are required for an intersubband transition to occur. Therefore, at low temperatures, when the phonon occupancy is small, intersubband transitions due to the emission of acoustic phonons of energy much greater than $k_B T_e$, are blocked by the Pauli exclusion.[50] This suggests an approximate subband decoupling scheme at low temperatures with energy relaxing mainly by small-angle intrasubband scattering.[14,50] Consequently the total energy loss rate can be approximated by $P \cong P_{11} + P_{22}$. When a hot electron undergoes an intrasubband transition by the emission of an acoustic phonon, the electron changes its momentum and at the same time it loses energy to the phonon. At low temperatures, the Fermi gas has a sharp boundary curve and consequently momentum changes, which involve the emission of an acoustic phonon of energy much greater than $k_B T_e$, are hindered greatly. Hence only small-angle scattering is allowed at very low temperatures.[49,50] Then, in the case under discussion, low-angle scattering should occur in the first subband, which is characterized by the dependencies $P_{11} \propto (T_e^5\text{-}T_L^5)$ for deformation potential scattering and $P_{11} \propto (T_e^3\text{-}T_L^3)$ for piezoelectric scattering.[14,49] In the case of samples with high carrier density, such that the Fermi level is well above the second subband energy E_2, the theory[14] predicts that the hot electrons in the second subband should also undergo low-angle scattering so that $P_{22} \propto (T_e^3\text{-}T_L^3)$ for piezoelectric scattering, but with a different proportionality constant A [see Eq. (7)] compared to that for the first subband. The fact that the density of carriers in the second subband is considerably smaller than that in the first subband (see Table I) is not so important because the power losses are not due to all the electrons in each subband, but rather due to the electrons within a narrow range of energies in the close vicinity of the Fermi level.[14,18]

For the modulation-doped $In_{0.53}Ga_{0.47}As/In_{0.52}Al_{0.48}As$ heterojunctions samples with $t_S = 100$ Å, we found that both P_{11} and P_{22} are indeed proportional to $(T_e^3\text{-}T_L^3)$ but with different values for the coefficient A (see Table I), in agreement with the theoretical predictions.[11,14] This is also true for the electron temperature dependencies of P_{22} and P_{11}, deter-

mined experimentally for the samples with $t_S=0$ and 200 Å, respectively. Therefore, it appears that in our samples with double-subband occupancy, the values found for the Fermi energy with respect to the bottom of the second subband (E_F-E_2) and the subband separation (E_2-E_1) are sufficiently large (see Table I), so that the intersubband scattering processes (P_{12} and P_{21}) can indeed be neglected and hence the energy loss rates from hot electrons in both populated subbands show the same electron temperature dependence as represented by Eq. (7) with $\gamma\cong 3$. This result is in contrast to the case of GaAs/$Ga_{1-x}Al_xAs$ heterojunctions with double-subband occupancy, where it was found[14,15] that the mean exponent γ, saturated at a value of about 2 when the Fermi energy was increased well above the bottom of the second subband, by using the persistent photoconductivity effect. The latter was explained[14,15] by assuming that the electrons in the second subband experience quasielastic scattering,[49] which is characterized by the dependence $P_{22}\propto(T_e$-$T_L)$. However, the observation of $\gamma\cong 2$ would also imply that the measurements were carried out over an intermediate regime (see Refs. 3,10,16,23).

The scattering of 2D electrons from ionized impurities, alloy disorder, interface roughness, and acoustic phonons, leads to broadening of Landau levels, which can be approximated by $\Gamma=\hbar/2\tau_q$.[28,33] Using the values obtained for the quantum lifetime τ_q of 2D electrons in the modulation-doped $In_{0.53}Ga_{0.47}As/In_{0.52}Al_{0.48}As$ heterojunctions (Table I) yields values in the range from 1.6 to 4.4 meV for Γ. The mean energy $\langle\hbar\omega\rangle$ of the acoustic phonons involved in the scattering process is estimated to be smaller than 1 meV in the temperature range of the measurements (see below). Therefore, the energy-level broadening in our samples is several times larger than the mean energy of acoustic phonons. This implies that the 2D behavior of the electron gas does not affect appreciably the electron acoustic phonon interaction;[4,30] the scattering of electrons from acoustic phonons can be treated as bulklike. Therefore, it is instructive to compare the results for energy loss rates determined experimentally for modulation-doped $In_{0.53}Ga_{0.47}As/In_{0.52}Al_{0.48}As$ heterojunctions with a theoretical model[3,16,21] based on the three-dimensional electron energy loss by piezoelectric and deformation potential scattering

$$P=f(T_e,T_L)(C_{np}+C_p)(k_BT_e-k_BT_L) \tag{9}$$

with

$$f(T_e,T_L)=\frac{\sinh(X_L-X_e)}{\sinh X_L-\sinh X_e}\left(\frac{X_LX_e}{X_L-X_e}\right), \tag{10}$$

$$C_{np}=3\Xi^2m^{*2}k_F/\pi\rho\hbar^3, \tag{11}$$

and

$$C_p=\frac{3e^2K_{av}^2m^{*2}V_S^2}{2\pi\epsilon_s\hbar^3k_F}. \tag{12}$$

Here $X_e=\langle\hbar\omega\rangle/2k_BT_e$, $X_L=\langle\hbar\omega\rangle/2k_BT_L$ and $\langle\hbar\omega\rangle=2^{1/2}\hbar V_Sk_F$. C_{np} and C_p are the magnitudes of the deformation potential (nonpolar acoustic) and the piezoelectric (polar acoustic) interactions, respectively, for a bulk material expressed in terms of the Fermi wave vector k_F and sound velocity V_S, and $\langle\hbar\omega\rangle$ is the acoustic phonon energy averaged over the Fermi surface. The function $f(T_e,T_L)$ approaches unity at high temperatures and falls exponentially at low temperatures. Equation (9) provides an approximation extending the high-temperature regime towards low temperatures.[3] The power loss, as given by Eq. (9), has been calculated using the values (Table I) determined experimentally for the effective mass, carrier density, and Fermi energy of 2D electrons in the modulation-doped $In_{0.53}Ga_{0.47}As/In_{0.52}Al_{0.48}As$ heterojunctions samples; the other physical parameters of bulk $In_{0.53}Ga_{0.47}As$ used in the calculations [sound velocity V_S ($=4810$ ms^{-1}), density $\rho(=5590$ kgm^{-3}), deformation potential Ξ ($=6.5$ eV), average electromechanical coupling constant K_{av}^2 ($=2.0\times10^{-3}$), and permittivity ϵ_s ($=13.77\epsilon_0$)] are taken from the literature.[17,51] Equation (9) fits reasonably to the experimental data for the first subband of the sample with $t_S=100$ Å [Fig. 9(a)], although not as good as that of Eq. (8). For the second subband, however, the power loss predicted by Eq. (9) is about an order of magnitude greater than that determined experimentally [Fig. 9(b)]. This indicates that the use of the bulk expression for calculation of the power loss from hot electrons in the second subband of our samples, is debatable. Furthermore, in contrast to Eq. (8), Eq. (9) predicts that the contributions of piezoelectric coupling and deformation-potential coupling to power loss are comparable with each other.

The energy relaxation time (τ_E) for intrasubband processes can be obtained from the power loss measurements for each populated subband using[3]

$$P=\frac{\langle\hbar\omega\rangle}{\tau_E}\frac{(k_BT_e-k_BT_L)}{k_BT_e}. \tag{13}$$

Figure 10 shows the energy-relaxation time as a function of electron temperature for the modulation-doped $In_{0.53}Ga_{0.47}As/In_{0.52}Al_{0.48}As$ heterojunction samples studied. The values obtained for τ_E fall in the range of values found previously, in the acoustic phonon regime, for GaAs/$Ga_{1-x}Al_xAs$ heterostructures (see for instance Refs. 3,7). Such large values of τ_E indicate that the energy loss mechanism in this temperature range is not so efficient and lead to the rapid rise of electron temperature when the input power is increased (see Fig. 8). However, as can be seen from Fig. 10, the energy relaxation due to acoustic phonons becomes faster at higher electron temperatures. Although τ_E shows a similar behavior with T_e for all the samples studied, its magnitude differs considerably from one sample to another, which may be a consequence of differences in the values of transport mobility and Fermi wave vector used in the calculations of the input power and the mean phonon energy, which are required to estimate the energy-relaxation time. The energy-relaxation times determined for the electrons in the first and second subbands of the sample with $t_S=100$ Å, are essentially the same for $(T_e$-$T_{L0})>2$ K (Fig. 10). This suggests that the two populated subbands behave as parallel channels for energy loss but with negligible inelastic inter-

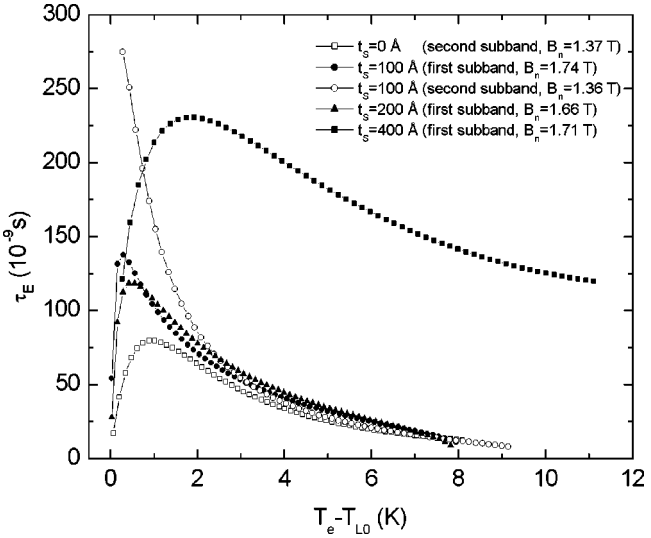

FIG. 10. Energy relaxation time (τ_e) versus T_e-T_{L0} for the modulation-doped $In_{0.53}Ga_{0.47}As/In_{0.52}Al_{0.48}As$ heterojunction samples studied. The full curves through the experimental data points are intended as a guide to the eye.

subband scattering. We also note that, for $(T_e$-$T_{L0})>2$ K, the energy-relaxation time determined for the sample with $t_S = 400$ Å, is much longer in comparison with those found for all the samples with double-subband occupancy. This result implies that the parallel conduction in the barrier of this sample has a considerable effect on energy relaxation.

IV. CONCLUSIONS

The energy loss rates, in the acoustic phonon regime, of 2D electrons in modulation-doped $In_{0.53}Ga_{0.47}As/In_{0.52}Al_{0.48}As$ heterojunction samples of single- and double-subband occupancy, have been investigated using Shubnikov-de Hass (SdH) effect measurements at lattice temperatures (T_L) between 3.3 and 15 K, and applied electric fields up to 120 Vm^{-1}. The electron temperature (T_e) has been determined from the changes in the amplitude of the SdH oscillations measured as functions of the lattice temperature and applied electric field. The electron temperatures determined separately for the first and second subbands are essentially the same; the electrons in both subbands are in thermal equilibrium with each other. For the samples with double-subband occupancy, the energy loss rate from the electrons in each subband to the lattice is proportional to $(T_e^3$-$T_L^3)$ but with different proportionality constants, in agreement with the theoretical predictions for power loss due to unscreened piezoelectric scattering.

ACKNOWLEDGMENTS

We are grateful to TÜBİTAK (TBAG-1676) and the Hacettepe University Research Fund (Project No. 99.02.602.004) for financial support.

[1] E. M. Conwell, *High Field Transport in Semiconductors*, Solid State Physics, Suppl. 9, edited by F. Seitz, D. Turnbull, and H. Ehrenreich (Academic, New York, 1967).
[2] S. A. Lyon, J. Lumin. **35**, 121 (1986).
[3] B. K. Ridley, Rep. Prog. Phys. **54**, 169 (1991).
[4] P. J. Price, J. Appl. Phys. **53**, 6863 (1982).
[5] S. Das Sarma, J. K. Jain, and R. Jalabert, Phys. Rev. B **37**, 6290 (1989).
[6] Y. Okuyama and N. Tokuda, Phys. Rev. B **40**, 9744 (1989).
[7] H. Sakaki, K. Hirakawa, J. Yoshino, S. P. Svensson, Y. Sekiguchi, T. Hotta, and S. Nishii, Surf. Sci. **142**, 306 (1984).
[8] M. Inoue, Superlattices Microstruct. **1**, 433 (1985).
[9] A. K. M. Wennberg, S. N. Ytterboe, C. M. Gould, H. M. Bozler, J. Klem, and H. Morkoc, Phys. Rev. B **34**, 4409 (1986).
[10] K. Hirakawa and H. Sakaki, Appl. Phys. Lett. **49**, 889 (1986).
[11] M. G. Blyumina, A. G. Denisov, T. A. Polyanskaya, I. G. Savel'ev, A. P. Senichkin, and Yu. V. Shmartsev, Pis'ma Zh. Éksp. Teor Fiz. **44**, 257 (1986) [JETP Lett. **44**, 331 (1986)].
[12] S. J. Manion, M. Artaki, M. A. Emanuel, J. J. Coleman, and K. Hess, Phys. Rev. B **35**, 9203 (1987).
[13] M. J. Barlow, B. K. Ridley, M. J. Kane, and S. J. Bass, Solid-State Electron. **31**, 501 (1988).
[14] A. M. Kreshchuk, M. Yu. Martisov, T. A. Polyanskaya, I. G. Savel'ev, I. I. Saidashev, A. Ya. Shik, and Yu. V. Shmartsev, Fiz. Tekh. Poluprovodn. **22**, 604 (1988) [Sov. Phys. Semicond. **22**, 377 (1988)].
[15] A. M. Kreshchuk, M. Yu. Martisov, T. A. Polyanskaya, I. G. Savel'ev, I. I. Saidashev, A. Ya. Shik, and Yu. V. Shmartsev, Solid State Commun. **65**, 1189 (1988).
[16] M. E. Daniels, B. K. Ridley, and M. Emeny, Solid-State Electron. **32**, 1207 (1989).
[17] A. Straw, A. J. Vickers, and J. S. Roberts, Solid-State Electron. **32**, 1539 (1989).
[18] D. R. Leadley, R. J. Nicholas, J. J. Harris, and C. T. Foxon, Semicond. Sci. Technol. **4**, 879 (1989); Solid-State Electron. **32**, 1473 (1989).
[19] R. Fletcher, J. J. Harris, C. T. Foxon, and R. Stoner, Phys. Rev. B **45**, 6659 (1992).
[20] K. Hirakawa, M. Grayson, D. C. Tsui, and Ç. Kurdak, Phys. Rev. B **47**, 16 651 (1993).
[21] N. Balkan, H. Çelik, A. J. Vickers, and M. Cankurtaran, Phys. Rev. B **52**, 17 210 (1995).
[22] Y. Ma, R. Fletcher, E. Zaremba, M. D'Iorio, C. T. Foxon, and J. J. Harris, Surf. Sci. **229**, 80 (1990).
[23] Y. Ma, R. Fletcher, E. Zaremba, M. D'Iorio, C. T. Foxon, and J. J. Harris, Phys. Rev. B **43**, 9033 (1991).
[24] H. Lobentanzer, W. W. Rühle, W. Stolz, and K. Ploog, Solid State Commun. **62**, 53 (1987).
[25] Y. Kodaira, H. Kuwano, and K. Tsubaki, Appl. Phys. Lett. **54**, 2414 (1989).
[26] M. Ç. Arikan, A. Straw, and N. Balkan, J. Appl. Phys. **74**, 6261 (1993).
[27] A. M. Kreshchuk, S. V. Novikov, I. G. Savel'ev, T. A. Polyanskaya, B. Pödör, G. Remenyi, and Gy. Kovacs, Acta Phys. Pol. A **94**, 415 (1998).

[28] H. Kahlert and G. Bauer, Phys. Status Solidi B **46**, 535 (1971).
[29] G. Bauer and H. Kahlert, Phys. Rev. B **5**, 566 (1972).
[30] T. Neugebauer and G. Landwehr, Phys. Rev. B **21**, 702 (1980).
[31] W. Hönlein and G. Landwehr, Surf. Sci. **113**, 260 (1982).
[32] T. Ando, J. Phys. Soc. Jpn. **37**, 1233 (1974).
[33] T. Ando, A. B. Fowler, and F. Stern, Rev. Mod. Phys. **54**, 437 (1982).
[34] A. Isihara and L. Smrcka, J. Phys. C **19**, 6777 (1986).
[35] P. T. Coleridge, R. Stoner, and R. Fletcher, Phys. Rev. B **39**, 1120 (1989).
[36] H. Çelik, M. Cankurtaran, A. Bayrakli, E. Tiras, and N. Balkan, Semicond. Sci. Technol. **12**, 389 (1997).
[37] D. R. Leadley, R. J. Nicholas, J. J. Harris, and C. T. Foxon, Semicond. Sci. Technol. **4**, 885 (1989).
[38] M. Hayne, A. Usher, J. J. Harris, and C. T. Foxon, Phys. Rev. B **46**, 9515 (1992).
[39] M. Cankurtaran, H. Celik, E. Tiras, A. Bayrakli, and N. Balkan, Phys. Status Solidi B **207**, 139 (1998).
[40] P. T. Coleridge, Semicond. Sci. Technol. **5**, 961 (1990).
[41] W. de Lange, Ph.D. thesis, Eindhoven University of Technology, Netherlands, 1993.
[42] D. R. Leadley, R. Fletcher, R. J. Nicholas, F. Tao, C. T. Foxon, and J. J. Harris, Phys. Rev. B **46**, 12 439 (1992).
[43] A. Kastalsky, R. Dingle, K. Y. Cheng, and A. Y. Cho, Appl. Phys. Lett. **41**, 274 (1982).
[44] E. Tiras, M. Cankurtaran, H. Çelik, A. Boland Thoms, and N. Balkan, Superlattices Microstruct. **29**, 147 (2001).
[45] R. Dingle, H. L. Störmer, A. C. Gossard, and W. Wiegmann, Surf. Sci. **98**, 90 (1980).
[46] K. Seeger, *Semiconductor Physics - An Introduction*, 6th ed. (Springer-Verlag, New York, 1997).
[47] S. Altinöz, E. Tiras, A. Bayrakli, H. Çelik, M. Cankurtaran, and N. Balkan, Phys. Status Solidi A **182**, 717 (2000).
[48] Sh. M. Kogan, Fiz. Tverd. Tela (Leningrad) **4**, 2474 (1962) [Sov. Phys. Solid State **4**, 1813 (1963)].
[49] V. Karpus, Fiz. Tekh. Poluprovodn. **22**, 439 (1988) [Sov. Phys. Semicond. **22**, 268 (1988)].
[50] P. K. Milsom and P. N. Butcher, Semicond. Sci. Technol. **1**, 58 (1986).
[51] T. P. Pearsall, *GaInAsP Alloy Semiconductors*, 1st ed. (Wiley, New York, 1982).